Applied Ocean Research 149 (2024) 104065

Contents lists available at ScienceDirect

Applied Ocean Research

journal homepage: www.elsevier.com/locate/apor

Research paper

Electricity forecast adapted to ocean conditions: The Mutriku case study

Isabel Casas [a,*], Jon Lekube [b]

[a] University of Deusto, Av. de las Universidades, 24, Bilbao, Spain
[b] Basque Energy Agency, Bilbao, Spain

ARTICLE INFO

Keywords:
Wave energy
Electricity forecast
Time series
Varying coefficients regression
Mutriku Wave Power Plant

ABSTRACT

It is essential for any wave power plant at the commercialising stage to accurately model and forecast its production to ensure a good functioning and an efficient trading in the daily wholesale electricity market. Altogether, a reliable forecast is a required step for the establishment of wave energy as a sustainable and viable source of electricity. We propose models whose coefficients adapt to the variation of ocean conditions and apply them to model/estimate and forecast the electricity production of two oscillating wave converters from the Mutriku Wave Power Plant during 2018. After a statistical analysis comparing different approaches, we recommend to model the production using a regression with coefficients depending on the wave height and to do short-term forecast using an autoregressive function with coefficients also depending on the wave height.

1. Introduction

Renewable energy development and implementation are now part of many countries' public policies. This also applies to wave energy, which is currently undergoing significant global expansion in research and development. In particular, there is an active field of research dedicated to improving and developing wave energy converters (WEC) to reach the commercialisation stage (see Foteinis (2022) for a detailed review). This paper focuses on modelling and forecasting energy production from WEC in the Mutriku Wave Power Plant (MWPP), providing an approach that should be transferable to other plants. The modelling part of our analysis will measure the efficiency of WEC in converting ocean energy into electricity. We also analyse and compare fourteen models' 13 to 36 h ahead forecast. Energy producers interested in trading energy in the daily European Electricity Market (EEM) will benefit from this forecast horizon, and we hope to contribute to the establishment of businesses or public entities managing wave power plants, aiding them in profiting from selling their energy production in the EEM.

The MWPP (Fig. 1), built and maintained by the Basque Energy Agency (EVE), utilises oscillating water columns (OWC) to convert the energy from the ocean into electricity. The MWPP stands out among wave power projects because it has been connected to the grid the longest, since July 2011 (Torre-Enciso et al., 2009, 2010).

Although limited research has been carried out in electricity forecast from waves due to the lack of commercialising plants data, the MWPP's one-hour energy production was first analysed by Ibarra-Berastegi et al. (2018) and Serras et al. (2019) for the period 2014–2016. The model in Serras et al. (2019) beat the random walk (RW) process for up to 19 h but not for longer horizons. Our objective is to provide a forecast model that beats the RW process for horizons of 13–36 h, so it is helpful to trade in the daily EEM. The installation of a new server in MWPP in 2018 allows us to analyse better quality data with a higher frequency and fewer missing values than previous studies.

Regarding data-driven statistical models, autoregressive (AR) models were often utilised for short-term forecasting ocean characteristics as in Paparella et al. (2015) and Guedes Soares and Cunha (2000) and for short-term forecast of WEC real-time control in Fusco and Ringwood (2010). Adding complexity, Jeon and Taylor (2016) show that autoregressive-mean average (ARMA) models with GARCH effects produce the best short-term forecast of wave power. In addition, studies have used time-varying coefficient linear models (TVLM) to forecast the wave energy flux (Reikard, 2009) and the power flow from different types of WEC (Reikard and Roger, 2011; Reikard et al., 2015). Lately, machine learning algorithms have been introduced in ocean engineering (Portillo Juan and Negro Valdecantos (2022) contains a comprehensive revision of this literature).

To the best of our knowledge, *functional coefficient* regressions are new to the energy field. For example, for the first time, Gao et al. (2021) and Chang et al. (2021) used panel data models with functional coefficients to explain changes in energy demand and forecast energy consumption at the macro level, respectively. In this paper, we propose using functional coefficient regressions to model the functioning of the

* Corresponding author.
E-mail address: icasas@deusto.es (I. Casas).

https://doi.org/10.1016/j.apor.2024.104065
Received 11 December 2023; Received in revised form 12 April 2024; Accepted 16 May 2024
Available online 28 May 2024
0141-1187/© 2024 The Authors. Published by Elsevier Ltd. This is an open access article under the CC BY-NC license (http://creativecommons.org/licenses/by-nc/4.0/).

(a) (b)

Fig. 1. (a) Exterior view of the Mutriku Wave Power Plant; (b) Interior view showcasing one of its turbines.

two OWCs and to forecast their energy production up to 36 h ahead. This model beats the RW and offers more accurate, helpful knowledge to trade in daily EEM.

In our modelling/estimation study, we compare ARMA-GARCH models, TVLMs, and functional coefficient linear models (FCLM) to explain the rate of ocean energy conversion into electricity of the MWPP's OWC in our dataset. We add machine learning models, such as the random forest, artificial neural networks and support vector machines, to the list of statistical methods in the forecast study. It is important to mention that our analysis may be extrapolated to other wave farms, other kinds of WECs, and other daily Electricity Markets.

This paper is organised as follows. We describe the data in Section 2 and the methodology in Section 3. The empirical analysis of the MWPP's data includes modelling the two OWC's efficiency, and their short-term forecast in Section 3.3. Finally, we draw conclusions in Section 4.

2. Data and methodology

2.1. Data description

The variable to model and forecast is the sum of the electricity production of two OWCs integrated with the breakwater at Mutriku Harbor (Torre-Enciso et al., 2009). In particular, this analysis has access to data from Turbines 7 and 8 that worked consistently between January 5, 2018 and December 31, 2018. Nominal power is recorded every half a second at MWPP, and we calculated its average over each hour to obtain the hourly energy production for the two turbines. The sum of both turbines production at hour t is denoted by $kWh_t = kWh_t^{T7} + kWh_t^{T8}$. We have 8,664 data points and a total generation of 63,348 kWh. The capacity factor, as defined in Izquierdo et al. (2010), is 20%. The capacity factor expression is:

$$CF = \frac{\text{63,348 kWh in 2018}}{\text{8,688 h} \times \text{37 kW nominal power}} = 0.197.$$

Ocean variables such as the spectral significant wave height ($H_{m0,t}$), spectral mean period ($T_{m02,t}$), tidal level ($Tide_t$), swell direction ($SwellDir_t$), wind speed ($WindSp_t$) and wind direction ($WindDir_t$) are common predictors of energy production and publicly available from Puertos del Estado (Spain's State Ports) website. This paper's ocean variables correspond to the SIMAR point number 3171032, which is closest to the MWPP's ocean site (map in Fig. 2). Puertos del Estado uses the WAM model to predict ocean variables at each SIMAR point from values at the Bilbao Buoy and the HARMONIE-AROME model to predict wind variables. The wave energy flux (WEF) at time t is calculated by

$$WEF_t = \frac{\rho g^2}{64\pi} H_{m0,t}^2 T_{m02,t} = 0.491 H_{m0,t}^2 T_{m02,t},$$

where g is the acceleration due to gravity and ρ is the water density. Missing values of the kWh series are replaced using the k-nearest-neighbor algorithm (Altman, 1992), which does not depend on the data time structure.

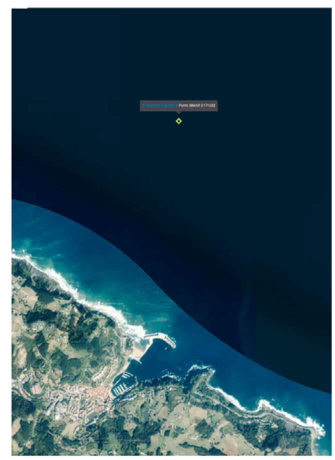

Fig. 2. Google map with Mutriku Wave Power Plant and SIMAR point number 3171032.

Figs. 3(a) and 4(a) show that the spectral significant wave height was lower than 2.5 m for more than 90% of the sample hours. However, it was lower than 0.5 m for only 4% of the sample hours and higher than 2.5 m for 7% of the sample hours. The spectral mean period was between 5 and 8 s for about half of the sample hours.

In 2018, at SIMAR point number 3171032, WEF values were ranged from a minimum of 0.07 kW/m to a maximum of 181.40 kW/m. The first quartile was 1.638 kW/m, the median was 4.263 kW/m, the mean was 9.04 kW/m, and the third quartile was 10.07 kW/m. Fig. 4(b) shows moderate values of the WEF, approximately between 10 and 50 kW/m, corresponded to the largest energy production values. The relationship between the WEF and energy production does not look linear. This is because the turbine damper closes when the pressure in the chamber is too high, which happens for largest waves.

Table 1 shows results from statistical tests to analyse the associations between energy production and ocean variables. Pearson's coefficient is significant for all variables except the swell direction. To test for non-linear associations, we run Kendall's test that shows a monotonic, not necessarily linear, association between energy production and the weave energy flux, significant wave height, wave period, wind speed and wind direction. However, we do not see any association between energy production and swell direction or between energy production and tidal level. Therefore, we discard these two ocean variables from the list of predictors. Besides, the scale of association between energy production and swell direction and between energy production and wind direction are minor, and these two are also discarded from the list of predictors. In light of these results, we chose the wave energy flux, significant wave height, spectral mean period, and wind speed as possible predictors of energy production in our analysis.

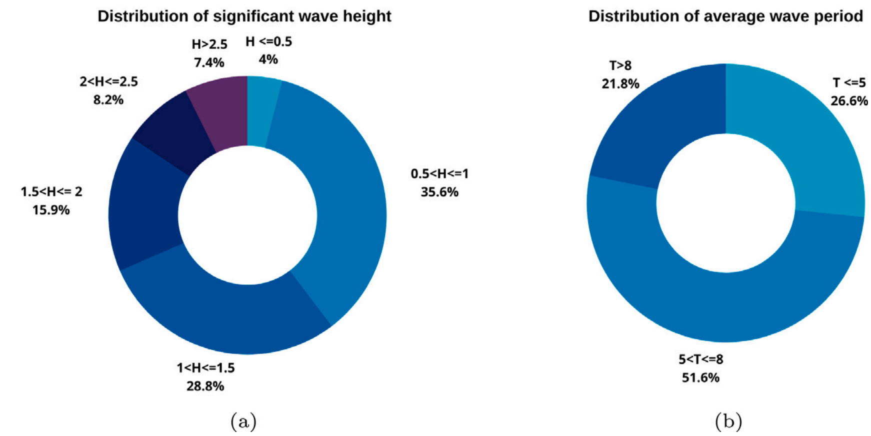

Fig. 3. Ring charts illustrating the distribution of (a) spectral wave height values and (b) spectral mean wave period, both at SIMAR point number 3171032 in 2018.

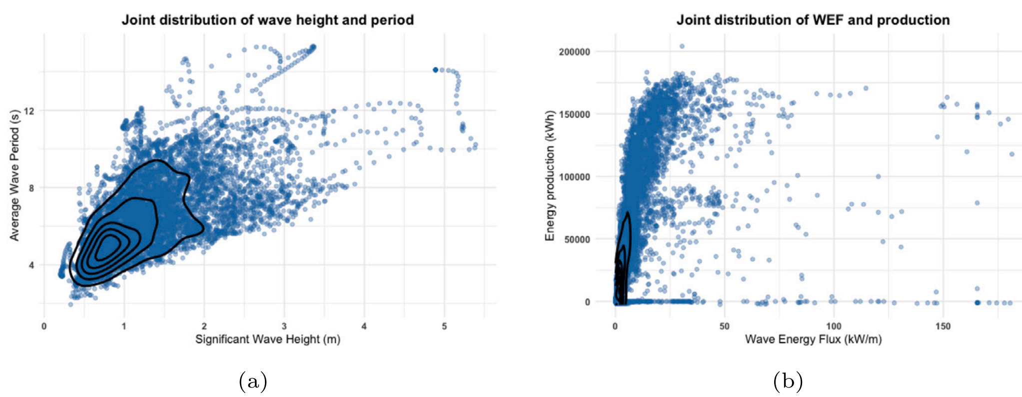

Fig. 4. Scatter plots illustrating the distribution of (a) significant wave height and spectral mean average period and (b) wave energy flux and energy production, both at SIMAR point number 3171032 during 2018.

Table 1
Pearson's and Kendall's correlation test results between energy production and ocean variables.

		Pearson		Kendall	
		ρ	p-value	τ	p-value
Wave energy flux	WEF	0.442	<0.001	0.606	<0.001
Spectral significant height	H_{m0}	0.691	<0.001	0.593	<0.001
Spectral mean Period	T_{m02}	0.568	<0.001	0.440	<0.001
Tidal level	$Tide$	−0.016	0.139	−0.009	0.221
Swell direction	$SwellDir$	0.097	<0.001	−0.005	0.510
Wind direction	$WindDir$	0.036	0.001	0.017	0.020
Wind speed	$WindSp$	0.280	<0.001	0.169	<0.001

A closer look at energy production and its autocorrelation function in Fig. 5 shows that its lowest values occur during June and July. This seasonal pattern is expected every year, but having only one year's data cannot be exploited in our analysis. To test for other seasonal patterns in our data, we use the R package (Ollech, 2019) that implements the WO-test described in Webel and Ollech (2018). The results conclude that our electricity production in 2018 is not seasonal.

A common source of misspecification for time series is violating the assumption of stationarity, which leads to spurious results in classical time series modelling (Engle and Granger, 1987). Fig. 5(c) illustrates the autocorrelation of kWh_t, indicating a slow decrease and suggesting high persistence in the process. This result allows us to test for unit roots in our production process. The unit root hypothesis is rejected via Augmented Dickey–Fuller tests with lags 1, 4, and 10 at a 5% significance level. Specifically, the t-statistics are −8.08, −8.21, and −6.19, respectively, all under the critical value of -1.96. On the other hand, the stationary process hypothesis is also rejected via Kwiatkowski–Phillips–Schmidt–Shin tests for lags 1, 4, and 10 at 5% significance level. Their statistics are 54.25, 22.44, and 10.81, respectively, all greater than the critical value of 0.463. Furthermore, the bottom right plot of Fig. 5(d) shows a significant partial correlation between current production and production up to 8 h before. This suggests the use of past values of productions as predictors of our current production (autoregressive process).

In summary, the statistical tests did not find evidence of seasonality in the kWh process, but its stationarity was not confirmed. It is reasonable to assume that this property transmits from ocean waves to the production process, the params of which will adapt to the type of turbine and ocean conditions. Varying coefficient autoregressive models are well suited in this context. Although the process may be non-stationary for the whole period, it is locally stationary, and its estimation using nonparametric kernel methods is asymptotically sound, as proven by Dahlhaus (2012).

3. Methodology

We want to understand how much ocean energy the MWPP's OWCs transform into electricity, as well as calculating their short-term future production forecast. We model energy production as a univariate time series using its lags and current ocean conditions as possible predictors.

3.1. Modelling

Although there is no causation between lagged production and current production, we can extract information from their correlations for better prediction. As in Guedes Soares and Cunha (2000), Fusco and

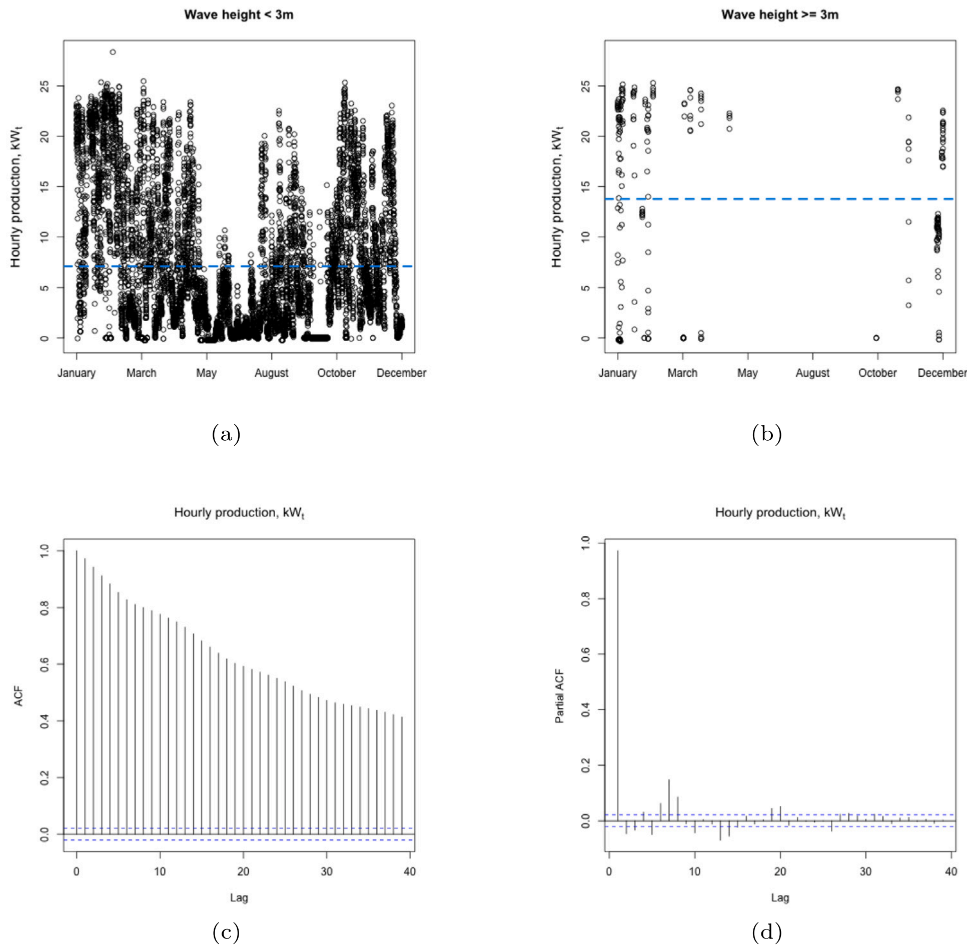

Fig. 5. (a) Scatter plot of Mutriku's hourly electricity production with significant wave height under 3 m; (b) same scatter plot with significant wave height over 3 m. The red lines in (a) and (b) represent the mean hourly electricity production. The bottom plots show (c) autocorrelation and (d) partial autocorrelation of hourly electricity production.

Ringwood (2010), Paparella et al. (2015) and Garcia-Abril et al. (2017), this property is represented with autoregressive (AR) or autoregressive with exogenous variables (ARX) models. The analysis in Jeon and Taylor (2016) shows that "the most accurate point and density forecasts overall were produced by the ARMA-GARCH models" when applied to WEF, even when compared with long-memory models. They also showed that using Gaussian error terms was good enough and that skewed or t-distributed error terms are unnecessary. Thus, we use the ARMA(r,m)-GARCH(p,q) model whose expression is:

$$kWh_t = \phi_0 + \sum_{i=1}^{r} \phi_i kWh_{t-i} - \sum_{j=1}^{m} \theta_j \varepsilon_{t-j} + u_t \tag{1}$$

$$\sigma_t^2 = \omega + \sum_{i=1}^{p} \alpha_i \sigma_{t-i}^2 + \sum_{j=1}^{q} \beta_j u_{t-j}^2 \tag{2}$$

$$u_t = \sigma_t \eta_t$$

where u_t is the innovation process at time $t = 1, 2, \ldots, T$; η_t is white noise; σ_t is the conditional standard deviation; and $\phi_i, \theta_j, \alpha_i, \beta_j$ are scalars that measure the linear relations between the current production and the variables on the right-hand side. When we add a function of ocean variables, X_t, to Eq. (1), we have the ARMAX(r,m)-GARCH(p,q) process. In our case, $X_t = (WEF_t, H_{m0,t}, T_{02,t}, WindSp_t)^\top$. Using the algorithm in Hyndman and Khandakar (2008) for our dataset to select the ARMA model lags, we found out that ARMA(3,4) is best suited for our problem. Therefore, we are using ARMA(3,4)-GARCH(1,1) and ARMAX(3,4)-GARCH(1,1) as part of the proposed estimation and forecasting models.

However, as some of these relations with the production may be non-linear, we also propose time-varying coefficient linear models (TVLM), which Reikard (2009) utilised to forecast the wave energy flux and Reikard and Roger (2011), Reikard et al. (2015) to forecast the power flow from different types of WEC. The TVLM is a very flexible approach, but its forecast is inconsistent because there is no information from the dependent variable at a future time. We argue that models whose coefficients adapt to variations in wave height, period, or tide level will provide a more accurate estimation and forecast of production than parametric models and even time-varying coefficient models. Therefore, we propose the functional coefficients linear model (FCLM), a multivariate regression whose coefficients may change according to a conditional variable Z changes. This semiparametric model is expressed by:

$$kWh_t = \mu(z_t) + \sum_{j=1}^{m} \delta_j(z_t)\, X_{jt} + \sum_{j=1}^{m} \sum_{i=1}^{p} \gamma_j(z_t)\, X_{j,t-i} + \varepsilon_t. \tag{3}$$

The coefficients $\mu(\cdot)$ and $\delta_j(\cdot)$ represent the relations between kWh_t and the right-hand side variables and ε_t is a random variable with mean zero and a constant variance. Note that adding lagged values of ocean conditions to the FCLM model would add information about ocean persistence. Unlike in parametric regression, $\mu(\cdot), \delta_j(\cdot)$ and $\gamma(\cdot)$ are not scalars, but unknown functions of a conditional variable, $Z = \{z_1, z_2, \ldots, z_T\}$. The TVLM has a representation like Eq. (3) for $z_t = t/T$.

The coefficients in Eq. (3) are estimated by combining ordinary least squares and the local polynomial kernel estimator, which was extensively studied in Fan and Gijbels (1996). Assuming that $\mu(\cdot)$

and $\delta_j(\cdot)$ are twice differentiable, the estimates resolve the following minimisation:

$$\arg\min_{\theta_0,\theta_1} \sum_{t=1}^{T} \left[kWh_t - X_t^\top\theta_0 - (z_t - z)x_t^\top\theta_1\right]^2 K_b(z_t - z). \quad (4)$$

These methodologies fit a set of weighted local regressions with an optimal chosen window size. The size of these windows is given by the bandwidth b, and the weights are given by the kernel $K_b(z_t - z) = b^{-1}K(\frac{z_t - z}{b})$. The choice of hyperparameter b is important because it defines the variability of the coefficient estimates. A large value of b will result in constant estimates of μ and δ_J. However, a small value will result in very variable estimates. In this paper, the bandwidth is selected automatically by leave-k-out cross-validation, Chu and Marron (1991), with $k = \lfloor T/4 \rfloor$ to ensure the independence of the subsamples. The asymptotic properties of these estimators for the TVLM are studied for $\{x_t, z_t, \epsilon_t\}$ iid or stationary processes in Cai et al. (2000); whereas Chang and Martinez-Chombo (2003), Cai et al. (2009), Sun et al. (2013) and Gao and Phillips (2013) have studied the case of non-stationary regressors or/and non-stationary z_t.

Seeking information from past values of production, Eq. (3) is extended to include p-lags of production. This model is the functional coefficients autoregressive-exogenous model (FCARX(p)) with the expression:

$$kWh_t = \mu(z_t) + \sum_{i=1}^{p} \beta_i(z_t)\ kWh_{t-i} + \sum_{j=1}^{m} \delta_j(z_t)\ X_{jt} + \epsilon_t. \quad (5)$$

The choice of optimal lag for the TVARX(p) and FCARX(p) models is calculated as in Yan et al. (2021) by:

$$\hat{p} = \arg\min_p (log RSS(p) + p\chi_T)$$

where $RSS(p) = \frac{1}{T}\sum_{t=1}^{T} \hat{\epsilon}_{t,p}^\top \hat{\epsilon}_{t,p}$ and χ_T is the penalty term whose natural choice is $\chi_T = \max(b_p^4, \frac{logT}{Tb_p})$. In our problem, the optimal value of p is 8. Therefore, we are proposing TVAR(8), TVARX(8), FCAR(8) and FCARX(8). One computing application with algorithms to estimate coefficients in Eqs. (3) and (5) is in R package *tvReg* described in Casas and Fernández-Casal (2022).

We do not add lags $X_{j,t-1}, \dots, X_{j,t-p}$ of ocean variables to Eq. (5), because their strong correlation with $kWh_{t-1}, \dots, kWh_{t-p}$ would cause multicollinearity in the context of a single equation and distortion of coefficient estimates.

3.2. Forecasting

It is vital for wave power plant operators to continually monitor and optimise the performance of OWCs to ensure the highest possible correlation in their production levels under varying ocean conditions, i.e., the rate of conversion of the OWCs. To do this, we fit the data to the modelling approaches suggested above and compare their estimation accuracy to select the best model.

We measure each model's estimation error with the root mean squared error (RMSE) and mean absolute error (MAE). Taking $\hat{r}_t$ as the residual at time t of our estimation, we define:

$$SE_t = \hat{r}_t^2 \qquad RMSE = \sqrt{\frac{1}{T}\sum_{t=1}^{T} SE_t},$$

$$AE_t = |\hat{r}_t| \qquad MAE = \frac{1}{T}\sum_{t=1}^{T} AE_t.$$

However, using the RMSE and MAE values to discriminate between models is too coarse as it considers the mean of the errors without accounting for their variance. The model confidence set (MCS) procedure by Hansen et al. (2011) is our workhorse for statistically discriminating between model performances. This procedure consists of a sequence of tests that permit the construction of a *set of superior models* (SSM), where the null hypothesis of equal predictive ability is not rejected at a certain confidence level (α). The procedure output is a set of p-values, one for each model, that, when compared with α, allows us to construct the SSM at $100(1-\alpha)$ confidence level.

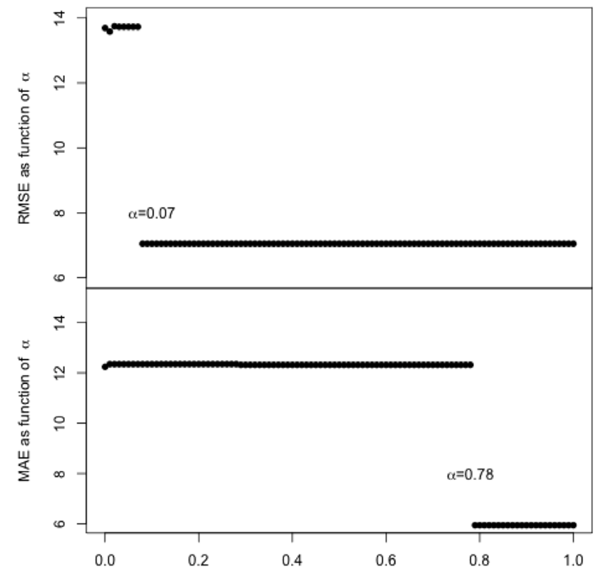

Fig. 6. Estimation errors as a function of confidence level. P-values of the MCS procedure greater than the confidence level (α) for the predictive values.

Table 2 displays the RMSE and MAE of each model and their p-values from the MCS procedure. One way to choose the best α and so find the relevant models included in the SSM is to plot the RMSE and MAE as a function of α: For each value of α, we calculate the RMSE and MAE of the average estimation of every model whose p-value is greater than α. Fig. 6 shows that the optimal confidence level is 93% ($\alpha = 0.07$) when using the RMSE and 30% ($\alpha = 0.7$) when using the MAE. Models with p-values ≥ 0.10 in the RMSE column and with p-values ≥ 0.7 in the MAE column are highlighted in bold in Table 2. The FCARX(8)|H is the only model that belongs to both optimal SSMs, and we choose it as the best model for estimating the sum of electricity production of the two OWCs at MWPP. This result suggests that current electricity production (kWh_t) is predicted by (i) production from the previous 8 h, (ii) current ocean conditions, and (iii) the spectral significant wave height conditions represented by the coefficients of this model. Figs. 9–7 show the coefficient estimates of the FCARX(8)|H.

Fig. 7(a) shows the estimation of the relationship between ocean energy and electricity production. The coefficient estimates for WEF significantly differ from zero at 5% level for waves up to 2 m. This relation-relatedness decreases overall with the increase of wave height and has no prediction power for waves over 2 m. The damper closes when too much pressure is in the air chamber, and the turbine stops producing energy. In addition, Fig. 7(b) indicates that wind speed significantly contributes to energy generation when waves are small. However, the 95% confidence bands include zero for waves over 1 m.

Fig. 8 illustrates the estimated production by the FCARX(8)|H for different combinations of wave height and period, while keeping the wind speed constant at its mean value of 4.5 m/s. The production at Mutriku Wave Power Plant (MWPP) is observed to increase with larger periods, reaching its peak around 3 m of wave height. However, production decreases steadily for larger waves beyond this point.

Fig. 9 displays the FCARX(8)|H coefficient estimates for kWh_{t-1}, kWh_{t-2}, kWh_{t-3} and kWh_{t-8}, along with their corresponding 95% confidence bands calculated using 10,000 bootstrap samples. In Fig. 9(a), the coefficient estimates for kWh_{t-1} are close to 1 for waves between 0.5 and 2 m, gradually decreasing for larger waves. This suggests that current electricity production is analogous to production from the

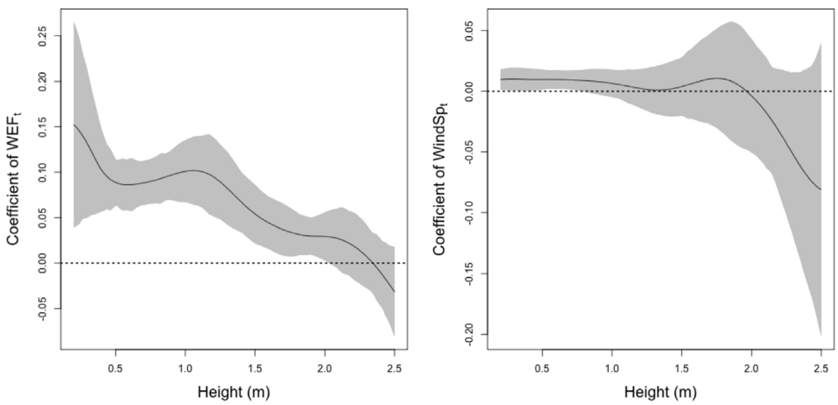

(a) (b)

Fig. 7. Plots illustrating the FCARX(8)|H coefficient estimates for (a) wave energy flux and (b) wind speed. The bands represent the 95% confidence interval calculated using 10,000 bootstrap samples.

Table 2
The RMSE and MAE of estimations and p-values from the MCS procedure for all competing models. The p-values of the relevant models are highlighted in bold. Specifically, p-values greater than 0.7 when considering the RMSE as the loss function, and greater than 0.07 when using the MAE as loss function.

	$RMSE$	MCS p-value	MAE	MCS p-value
Constant coefficients				
AR(8)	1.618	0.001	0.818	<0.001
ARX(8)	1.593	0.016	0.819	<0.001
ARMA(3,4)-GARCH(1,1)	1.659	0.004	0.781	**0.786**
ARMAX(3,4)-GARCH(1,1)	1.801	0.016	0.867	0.001
Time-varying coefficients				
TVLM	4.326	<0.001	3.106	<0.001
TVAR(8)	1.574	0.016	0.807	0.001
TVARX(8)	1.522	**0.072**	0.789	0.283
Coefficients conditional to the wave height				
FCLM|H	3.997	<0.001	2.756	<0.001
FCAR(8)|H	1.489	**0.072**	0.776	**1.000**
FCARX(8)|H	1.473	**1.000**	0.777	**0.786**
Coefficients conditional to the wave period				
FCLM|T	4.079	<0.001	2.807	<0.001
FCAR(8)|T	1.562	0.016	0.786	0.286
FCARX(8)|T	1.543	0.020	0.789	0.130

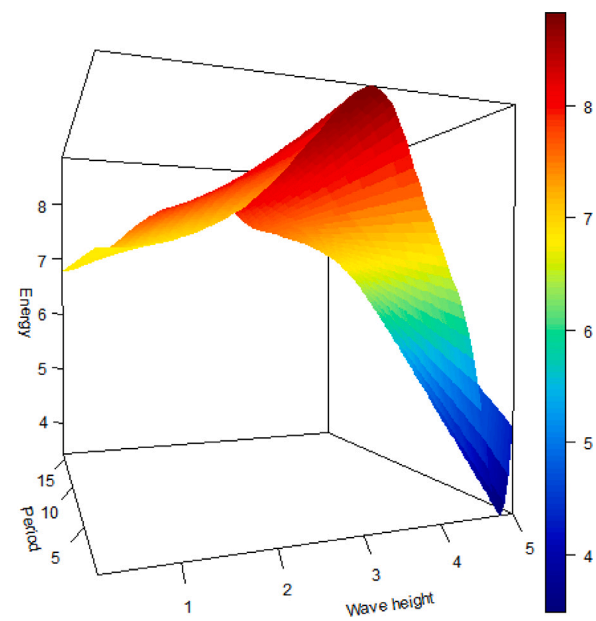

Fig. 8. Evolution of Mutriku's production explained by FCARX(8)|H across varying wave height and period values while keeping the wind speed constant at its mean value (4.5 m/s).

previous hour for waves of that magnitude. Similarly, the coefficient estimates for kWh_{t-2} and kWh_{t-3}, shown in Figs. 9(b) and (c) respectively, indicate that production from two and three hours prior are predictors of current production for waves under 1 m. However, larger lagged productions are not significant predictors of current production.

3.3. Optimising Mutriku's production forecasting

Electricity markets across 23 European countries in 2023 operate under a common regulation, allowing trade through 12 Nominated Electricity Market Operators (NEMO). These NEMOs conduct auctions for daily, intraday, and continuous markets. For a wave power plant like MWPP, accurate production forecasts are crucial for optimal participation in the spot market.

Fig. 10 illustrates the trading hours in the Iberian spot market, reflecting what would be the trading periods for MWPP's production. Producers quote the expected energy generation for each hour of the next day, 13 to 36 h in advance. A reliable forecast enhances a producer's ability to maximise benefits in the spot market.

In a related study (Ibarra-Berastegi et al., 2015), Random Forests (RF) improved wave energy forecast accuracy for short horizons. However, the study did not explore this improvement in the context of electricity production. The study establishes the Random Walk (RW) as the benchmark model for electricity production forecasting:

$$kWh^*_{T+h} = kWh_T + u_{T+h}, \qquad h = 1, 2, \ldots \tag{6}$$

The RW assumes unpredictability, forecasting the production at horizon h as $\widehat{kWh}^*_{T+h} = kWh_T$.

The analysis focuses on the 13- to 36-h forecasts of the sum production of Turbines 7 and 8 at MWPP. The training sample spans from January 5 to June 30, 2018, with the forecast sample starting on July 1, 2018, and ending on December 31, 2018. The algorithm used to calculate this forecast is as follows:

1. Collect the 1 to 36 h ahead forecast of ocean variables ($X^*_{T+k+1}, \ldots, X^*_{T+k+36}$), including the conditional variable ($z^*_{T+k+1}, \ldots, z^*_{T+k+36}$) at 11 am. These may be found on meteorological websites.
2. Produce an h-hour ahead forecast recursively for horizons $h = 1, 2, \ldots, 36$, but only keep the last 24 h (i.e., for $h2 = 13, 14, \ldots, 36$).

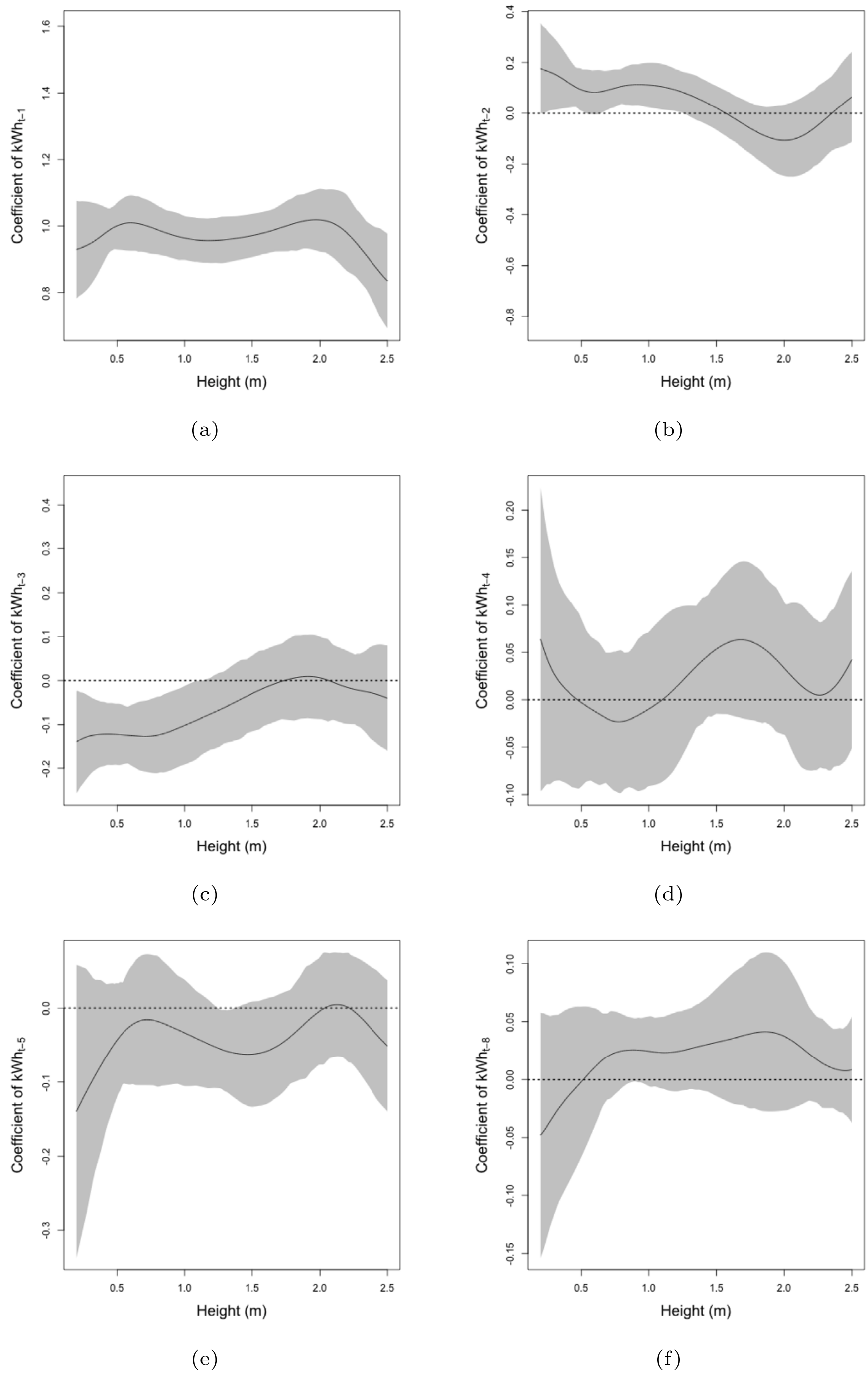

Fig. 9. Plots illustrating the FCARX(8)|H coefficient estimates for (a) kWh_{t-1}, (b) kWh_{t-2}, (c) kWh_{t-3}, (d) kWh_{t-4}, (e) kWh_{t-5}, and (f) kWh_{t-8}. The bands represent the 95% confidence interval calculated using 10,000 bootstrap samples.

3. Calculate the forecast errors for each horizon h_2 ($fe_k = kWh_{T+k+h_2} - \widehat{kWh}^*_{T+k+h_2}$), as well as the forecast squared errors ($fse_k = fe_k^2$) and forecast absolute errors ($fae_k = |fe_k|$)
4. Repeat Steps 1–3 for $k = 0, \dots, 4213$ times.
5. Use fse_k and fae_k to compare model performance using the MCS algorithm and report the forecast root mean squared error (FRMSE) and the forecast mean absolute error (FMAE).

Table 3 presents the FRMSE, FMAE, and p-values from the MCS procedure, comparing different models for the entire out-of-sample. Fig. 11 shows how models with p-values above $\alpha = 0.61$ experience a significant decrease in their FRMSE, and models with p-values above $\alpha = 0.46$ experience a significant decrease in the ir FMAE. The FCLM|H emerges as the top performer in forecasting electricity production for short-term horizons, ranking highest among all models using both forecast accuracy measures. Although, at a 40% confidence level, its forecast performance is not statistically different from the forecast performance of the RF, SVM models, and the BRNN when using the FRMSE to measure forecast errors. Nevertheless, this study

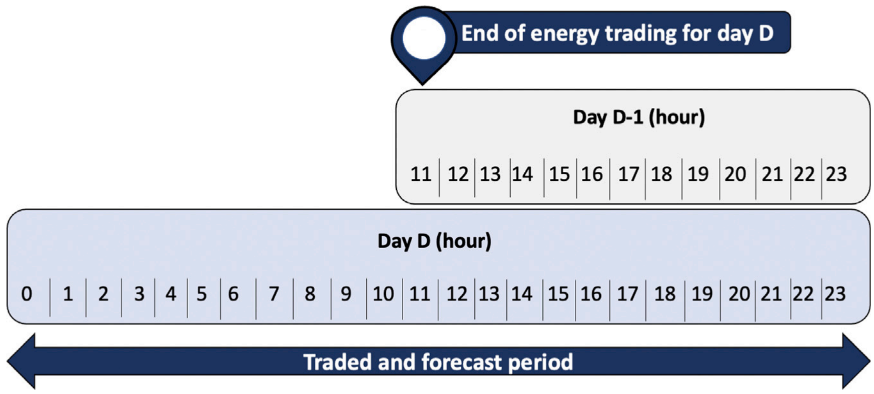

Fig. 10. Timeline in the daily Iberian electricity market trading.

Table 3
The FRMSE and FMAE of forecasts and p-values from the MCS procedure for all competing models. The p-values of the relevant models are highlighted in bold. Specifically, p-values greater than 0.61 when considering the RMSE as the loss function, and greater than 0.46 when using the MAE as loss function.

	FRMSE	MCS	FMAE	MCS
Benchmark				
RW	3.039	0.248	1.981	0.176
Constant coefficients				
ARMA(3,4)-Garch(1,1)	4.551	0.248	3.186	0.176
ARMA(3,4)-GJR(1,1)	4.553	0.248	3.188	0.176
Time-varying coefficients				
TVLM	2.395	0.310	1.551	0.176
TVAR(8)	13829173.501	0.248	599 548.906	0.176
TVARX(8)	15870750.541	0.248	36.913	0.176
Coefficients conditional to the wave height and period				
FCLM|Height	2.008	**1.000**	1.353	**1.000**
FCLM|Period	2.050	0.602	1.388	0.454
FCARX(8)|Height	3.449	0.248	2.413	0.176
FCARX(8)|Period	3.353	0.248	2.345	0.176
Machine learning				
RF	2.083	0.490	1.427	0.176
MLP	2.543	0.248	1.889	0.176
BRNN	2.047	0.602	1.390	0.454
SVM Linear	2.104	0.490	1.513	0.176
SVM Radial	2.095	0.490	1.400	0.454

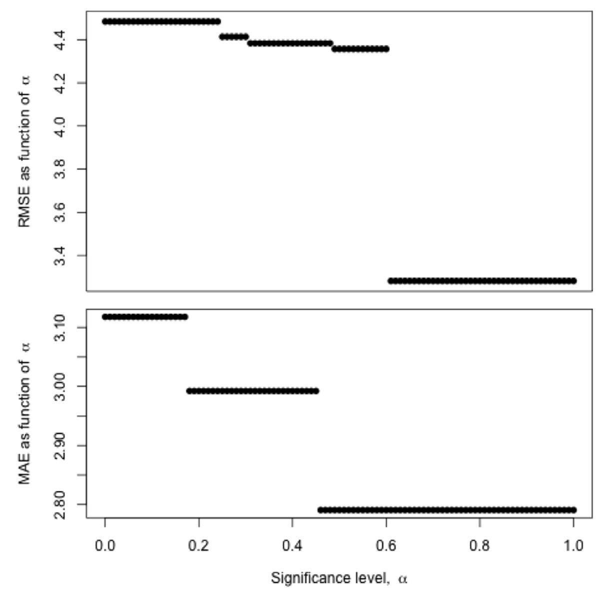

Fig. 11. Forecasting errors as a function of the confidence level.

recommends adopting the FCLM|H for production forecasting due to its interpretability and superior performance.

4. Conclusions

In this study, we conducted a comprehensive analysis of wave power plant operations, focusing on estimating and forecasting electricity production from two OWCs at MWPP. Our research aimed to optimise performance assessment under varying ocean conditions and provide practical insights for wave energy industry stakeholders.

The application of various modelling approaches, including AR, ARX, ARMA-GARCH, time-varying coefficient models, and the proposed functional coefficient models showed the FCARX(8)|H model as the most reliable for estimating electricity production.

In the forecasting phase, our attention shifted to predicting electricity production for short-term horizons, which is crucial for electricity market trading. The persistence model (RW) served as a benchmark, and our findings revealed that the FCLM|H model outperformed the RW and other sophisticated models regarding forecast accuracy.

While this study enhances our understanding of wave power plant operations, there is space for future research. Exploring long-term forecasting, incorporating additional environmental factors, and considering multiple OWCs simultaneously could further refine predictive models.

CRediT authorship contribution statement

Isabel Casas: Writing – review & editing, Writing – original draft, Visualization, Validation, Software, Resources, Project administration, Methodology, Formal analysis, Data curation, Conceptualization. **Jon Lekube:** Resources, Conceptualization.

Declaration of competing interest

The authors declare the following financial interests/personal relationships which may be considered as potential competing interests: Isabel Casas reports financial support was provided by Danish Independent Research Fund (grant no. 8142-00010B). Isabel Casas reports financial support was provided by Carlsberg Foundation grant no. CF19-0164. If there are other authors, they declare that they have no known competing financial interests or personal relationships that could have appeared to influence the work reported in this paper.

Data availability

Data will be made available on request.

Declaration of Generative AI and AI-assisted technologies in the writing process

During the preparation of this work the authors used ChatGPT in order to improve readability and language. After using this tool/service, the authors reviewed and edited the content as needed and take full responsibility for the content of the publication.

Acknowledgements

The authors would like to thank Puertos del Estado for providing the ocean data and EVE for providing the Mutriku Wave Power Plant data. Further thanks to Mikel Lezaun and the University of the Basque Country for hosting the first author during this project. The first author acknowledges financial support from the Danish Independent Research Fund (grant no. 8142-00010B) and the Carlsberg Foundation, Denmark (grant no. CF19-0164).

References

Altman, N., 1992. An introduction to kernel and nearest-neighborg nonparametric regression. Amer. Statist. 46 (3), 175–185.

Cai, Z., Fan, J., Yao, Q., 2000. Functional-coefficient regression models for nonlinear time series. J. Amer. Statist. Assoc. 95, 941–956.

Cai, Z., Li, Q., Park, J.Y., 2009. Functional-coefficient models for nonstationary time series data. J. Econometrics 148, 101–113.

Casas, I., Fernández-Casal, R., 2022. The R journal: tvReg: Time-varying coefficients in multi-equation regression in R. R J. 14, 79–100. http://dx.doi.org/10.32614/RJ-2022-002.

Chang, Y., Choi, Y., Kim, C.S., Miller, J.I., Park, Y.J., 2021. Forecasting regional long-run energy demand: A functional coefficient panel approach. Energy Econ. 96, 105117. http://dx.doi.org/10.1016/j.eneco.2021.105117.

Chang, Y., Martinez-Chombo, E., 2003. Electricity Demand Analysis Using Cointegration and Error-Correction Models with Time Varying Parameters: The Mexican Case. Working papers, Rice University, Department of Economics, URL https://ideas.repec.org/p/ecl/riceco/2003-08.html.

Chu, C.K., Marron, J.S., 1991. Comparison of two bandwidth selectors with dependent errors. Ann. Statist. 19, 1906–1918.

Dahlhaus, R., 2012. 13 - Locally stationary processes. In: Subba Rao, T., Subba Rao, S., Rao, C. (Eds.), Time Series Analysis: Methods and Applications. In: Handbook of Statistics, vol. 30, Elsevier, pp. 351–413.

Engle, R.F., Granger, C.W.J., 1987. Co-integration and error correction: Representation, estimation and testing. Econometrica 55 (2), 251–276.

Fan, J., Gijbels, I., 1996. Local polynomial modelling and its applications. In: Monographs on Statistics and Applied Probability Series, Chapman & Hall.

Foteinis, S., 2022. Wave energy converters in low energy seas: Current state and opportunities. Renew. Sustain. Energy Rev. 162, 112448. http://dx.doi.org/10.1016/j.rser.2022.112448.

Fusco, F., Ringwood, J.V., 2010. Short-term wave forecasting for real-time control of wave energy converters. IEEE Trans. Sustain. Energy 1, 99–106.

Gao, J., Peng, B., Smyth, R., 2021. On income and price elasticities for energy demand: a panel data study. Energy Econ. 96, http://dx.doi.org/10.1016/j.eneco.2021.105168.

Gao, J., Phillips, P.C.B., 2013. Functional Coefficient Nonstationary Regression. Tech. rep., Cowles Foundation Discussion Paper NO. 1911.

Garcia-Abril, M., Paparella, F., Ringwood, J., 2017. Excitation force estimation and forecasting for wave energy applications. IFAC-PapersOnLine 50 (1), 14692–14697, 20th IFAC World Congress.

Guedes Soares, C., Cunha, C., 2000. Bivariate autoregressive models for the time series of significant wave height and mean period. Coast. Eng. 40, 297–311.

Hansen, P.R., Lunde, A., Nason, J.M., 2011. The model confidence set. Econometrica 79, 453–497.

Hyndman, R.J., Khandakar, Y., 2008. Automatic time series forecasting: The forecast package for R. J. Stat. Softw. 27, 1–22.

Ibarra-Berastegi, G., Sáenz, J., Esnaola, G., Ezcurra, A., 2015. Short-term forecasting of the wave energy flux: analogues, random forests, and physics-based models. Ocean Eng. 104, 530–539.

Ibarra-Berastegi, G., Sáenz, J., Ulazia, A., Serras, P., Esnaola, G., Garcia-Soto, C., 2018. Electricity production, capacity factor, and plant efficiency index at the Mutriku wave farm (2014–2016). Ocean Eng. 147, 20–29.

Izquierdo, S., Montañés, C., Dopazo, C., Fueyo, N., 2010. Analysis of CSP plants for the definition of energy policies: The influence on electricity cost of solar multiples, capacity factors and energy storage. Energy Policy 38 (10), 6215–6221.

Jeon, J., Taylor, J.W., 2016. Short-term density forecasting of wave energy using ARMA-GARCH models and kernel density estimation. Int. J. Forecast. 32 (3), 991–1004. http://dx.doi.org/10.1016/j.ijforecast.2015.11.003, URL https://www.sciencedirect.com/science/article/pii/S0169207015001387.

Ollech, D., 2019. seastests: Seasonality tests. URL https://CRAN.R-project.org/package=seastests. R package version 0.14.2.

Paparella, F., Monk, K., Winands, V., Lopes, M.F.P., Conley, D., V. Ringwood, J., 2015. Up-wave and autoregressive methods for short-term wave forecasting for an oscillating water column. IEEE Trans. Sustain. Energy 6, 171–178.

Portillo Juan, N., Negro Valdecantos, V., 2022. Review of the application of Artificial Neural Networks in ocean engineering. Ocean Eng. 259, 111947.

Reikard, G., 2009. Forecasting ocean wave energy: Tests of time-series models. Ocean Eng. 36, 348–356.

Reikard, G., Robertson, B., Buckham, B., Bidlot, J.-R., Hiles, C., 2015. Simulating and forecasting ocean wave energy in Western Canada. Ocean Eng. 103, 223–236.

Reikard, G., Roger, W., 2011. Forecasting ocean waves: Comparing a physics-based model with statistical models. Coast. Eng. 58, 409–416.

Serras, P., Ibarra-Berastegi, G., Sáenz, J., Ulazia, A., 2019. Combining random forests and physics-based models to forecast the electricity generated by ocean waves: A case study of the Mutriku wave farm. Ocean Eng. 189, 106314.

Sun, Y., Cai, Z., Li, Q., 2013. Semiparametric functional coefficient models with integrated covariates. Econometric Theory 29, 659–672.

Torre-Enciso, Y., Marqués, J., López de Aguileta, L., 2010. Mutriku. Lessons learnt. In: Proceedings of the 3rd International Conference on Ocean Energy.

Torre-Enciso, Y., Ortubia, I., De Aguileta, L.L., Marqués, J., 2009. Mutriku wave power plant: from the thinking out to the reality. In: Proceedings of the 8th European Wave and Tidal Energy Conference, Uppsala, Sweden. Vol. 710, pp. 319–329.

Webel, K., Ollech, D., 2018. An overall seasonality test based on recursive feature elimination in conditional random forests. In: Proceedings of the 5th International Conference on Time Series and Forecasting. pp. 20–31.

Yan, Y., Gao, J., Peng, B., 2021. On time-varying VAR models: Estimation, testing and impulse response analysis. http://dx.doi.org/10.48550/ARXIV.2111.00450, arXiv. URL https://arxiv.org/abs/2111.00450.